News on MQXF magnet assembly

S. Izquierdo, J. Ferradas, P. Quassolo, A. Milanese, N. Lusa, S. Triquet, S. Straarup, M. Guinchard, S. Mugnier, K. Kandemir

… and many more. On behalf of the full MQXF team!

Previous session: https://indico.cern.ch/event/1177429/

CERN, 14 December 2022

CONTENTS

- MQXFB:
  - MQXFB02 Cold test results (Focus on mechanics)
  - Highlights on MQXFBMT4 magnet assembly

- MQXFS:
  - MQXFS7g magnet assembly.
  - MQXFS8 magnet assembly.

CONTENTS

- MQXFB:
  - **MQXFB02 Cold test results (Focus on mechanics)**
  - Highlights on MQXFBMT4 magnet assembly

- MQXFS:
  - MQXFS7g magnet assembly.
  - MQXFS8 magnet assembly.

MQXFB02 – Cold tests

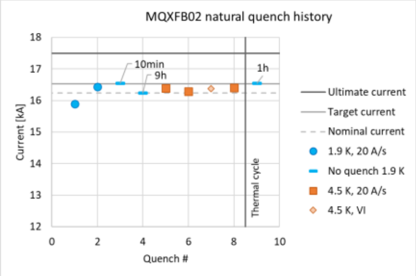

- **100% of the mechanical instrumentation** (Optical for coils and Electrical for rods) is **working well** at 1.9 K and during the powering phases.
  See https://indico.cern.ch/event/1213692/

- **Larger** winding pole **unloading** in **LE** and **RE** measurement locations. **Consistent** with expectations (**larger** coil size / **pre-load** in the **middle** of the coils).

- Target pre-load attained. Unloading at ~ 0.9 – 0.95 I_{nom}

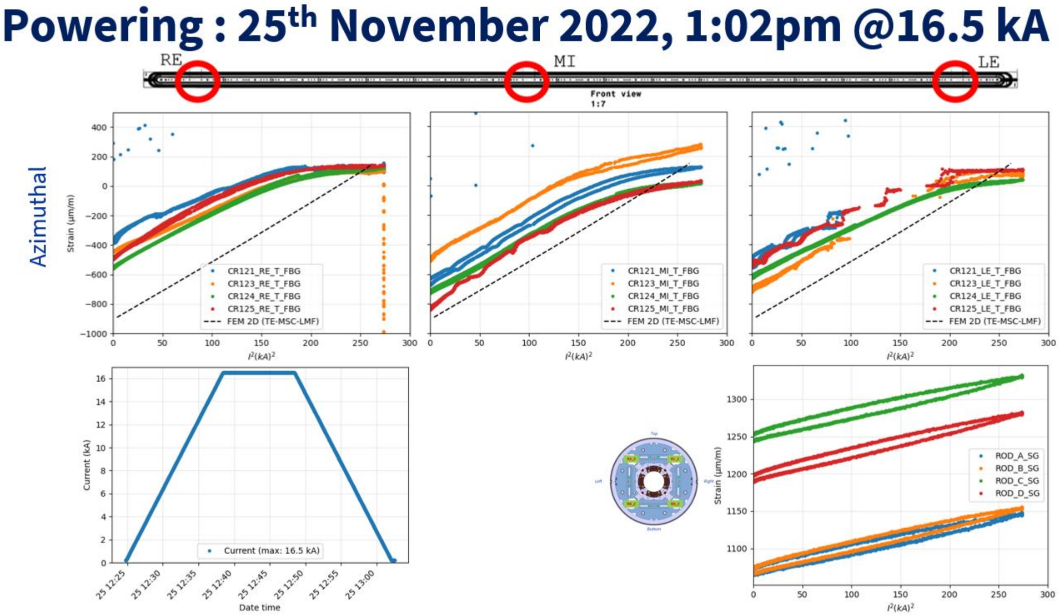

M. Guinchard, S. Mugnier and K. Kandemir

MQXFB02 – Cold tests

- **Axial rods** behaviour at **cold in line** with **MQXFBP3**.

		Δ Rod Strain CD FEM [με]	Δ Rod Strain 16.23 kA FEM [με]	Δ Rod Strain CD [με]	Δ Rod Strain 16.23 kA [με]
Magnet	MQXFBP1	670	35	452	70
	MQXFBP2			461	55
	MQXFBP3			517	75
	MQXFB02			571	~ 75

Comparison to FE model:

Regarding the magnet cool-down, final rod tension is 15 % lower than expected.

Magnet globally behaves as iron. Rods increase their tension at cold.

What could help to come closer to measurements? Lower friction or lower long. stiffness of the structure.

During energization: larger elongation than predicted by the numerical model. Still, this is very low, in terms of electromagnetic forces we see 5% of F_z during powering vs 2% we expect to see based on ANSYS.

What could help to come closer to measurements? Lower friction or lower long. stiffness of the structure.

CONTENTS

- MQXFB:
  - MQXFB02 Cold test results (Focus on mechanics)
  - **Highlights on MQXFBMT4 magnet assembly**

- MQXFS:
  - MQXFS7g magnet assembly.
  - MQXFS8 magnet assembly.

MQXFBMT4 – Assembly

- **MQXFBMT4 assembled** with **3** (non-virgin) **coils** from **MQXFBP1** and **CR127** (Virgin).
- Shimming plan defined based on the virgin coil measurements for all coils, targeting for the best geometrical compensation at cryogenic temperature. We assume a consistent decrease in size for the new coil.

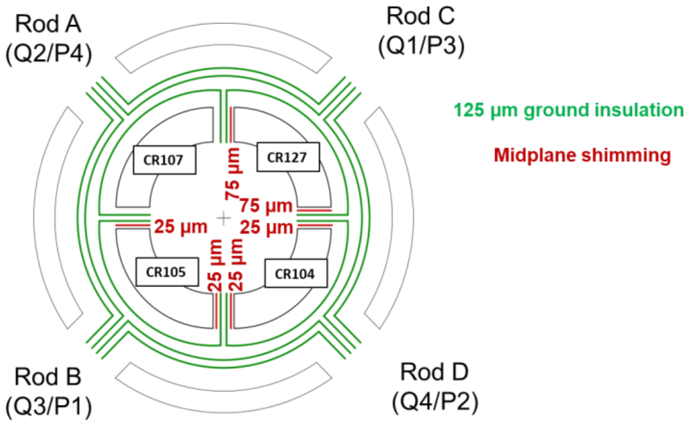

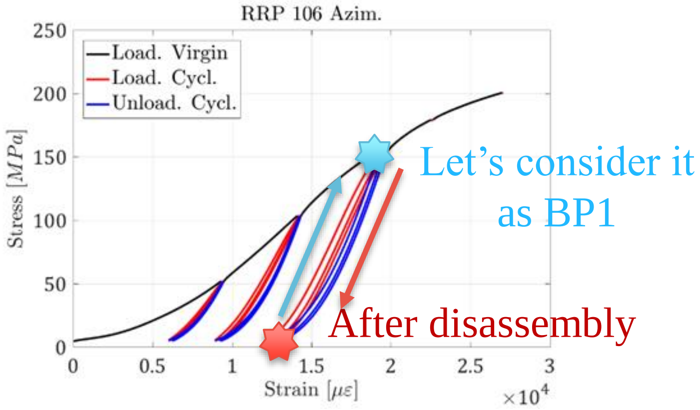

G. Vallone, M. Guinchard et al.

MQXFBMT4 – Assembly

- Coilpack **centering performed successfully** (all operations went **smoothly**).
- Magnet pre-loading (as well) smooth up to the insertion of the 13.7 mm loading keys.
- Then, **bladder failure** occurred at **390 bar**, when preparing for the insertion of the last 13.8 mm keys.
  - All **13.7 mm keys** were **in place** at the moment of the failure. All bladder **circuits** were **connected ensuring continuity** along the magnet longitudinal axis.
  - Failure mode indicate that the **bladder** was **out** of the **masters** (not supported). Positioning was checked before starting the loading. A second bladder was replaced preventively for the same reason.

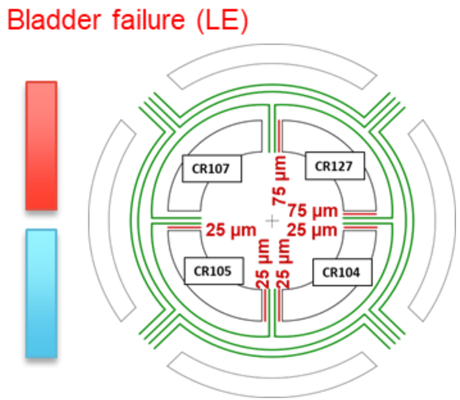

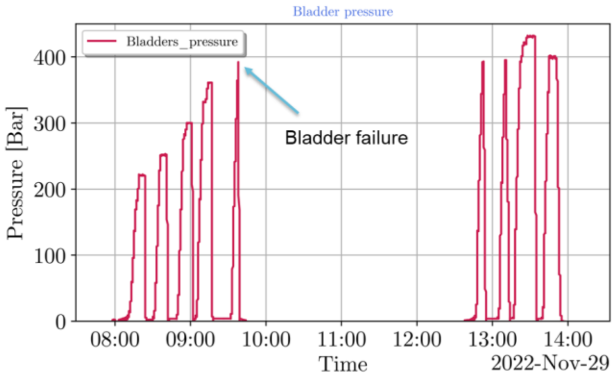

MQXFBMT4 – Assembly

- **Fast** mechanical **transient** as a result of the **sudden** (and local) **drop** in **pressure**.
  - Increase in comp. az. strain for CR107 and CR104 (diametrically opposite). Inverse effect for CR127 and CR105. Nothing seen on the RE side, covered by a different bladder.
  - The strain/spread among coils increases (up to a factor of 2 in the MI station) after the failure.

LE - ε_θ

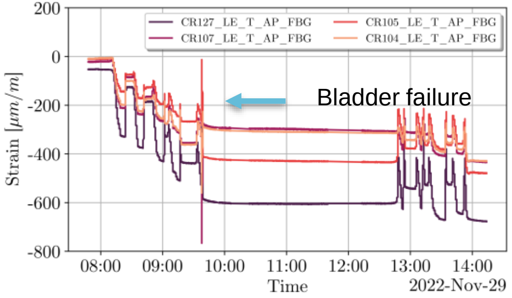

MI - ε_θ

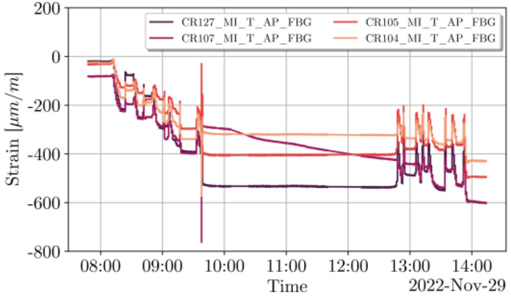

RE - ε_θ

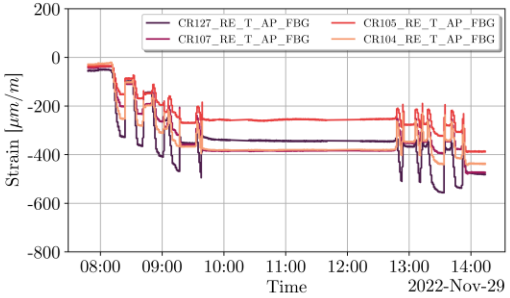

LE - ε_z

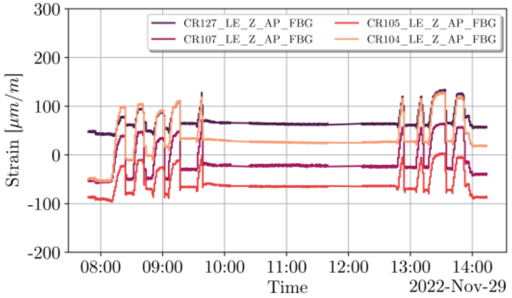

MI - ε_z

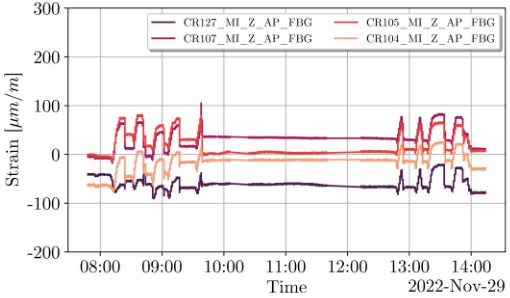

RE - ε_z

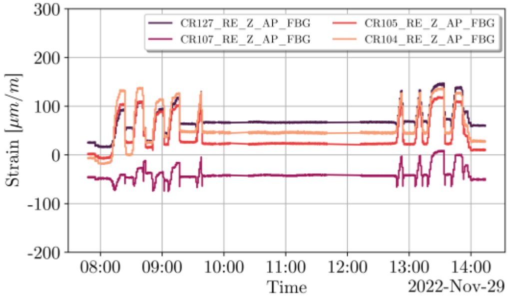

M. Guinchard, S. Mugnier, K. Kandemir

MQXFBMT4 – Assembly

- Non-Conformity report for the bladder failure in EDMS 2803022.
- **Two** bladder **cycles** up to **390 bar** performed upon restart of the pre-loading operations. **Half** of the created **imbalance** among coils could be **recovered** (see previous slide).
- **Loading completed** with the insertion of 13.8 mm keys. Magnet is **within specifications except** for the coil **peak stress**. The latter happens in CR107, which has already seen larger stress values during MQXFBP1 assembly and cold test.
  - **Average shell** stress (three stations): 58 MPa - Target: **+58** ± 6 MPa
  - **Average coil stress** (winding pole, three stations): -71 MPa - Target **-70** ± 10 MPa
  - **Peak coil stress** (winding pole, three stations): -107 MPa - Target **-100 MPa**

MQXFBMT4 – Assembly

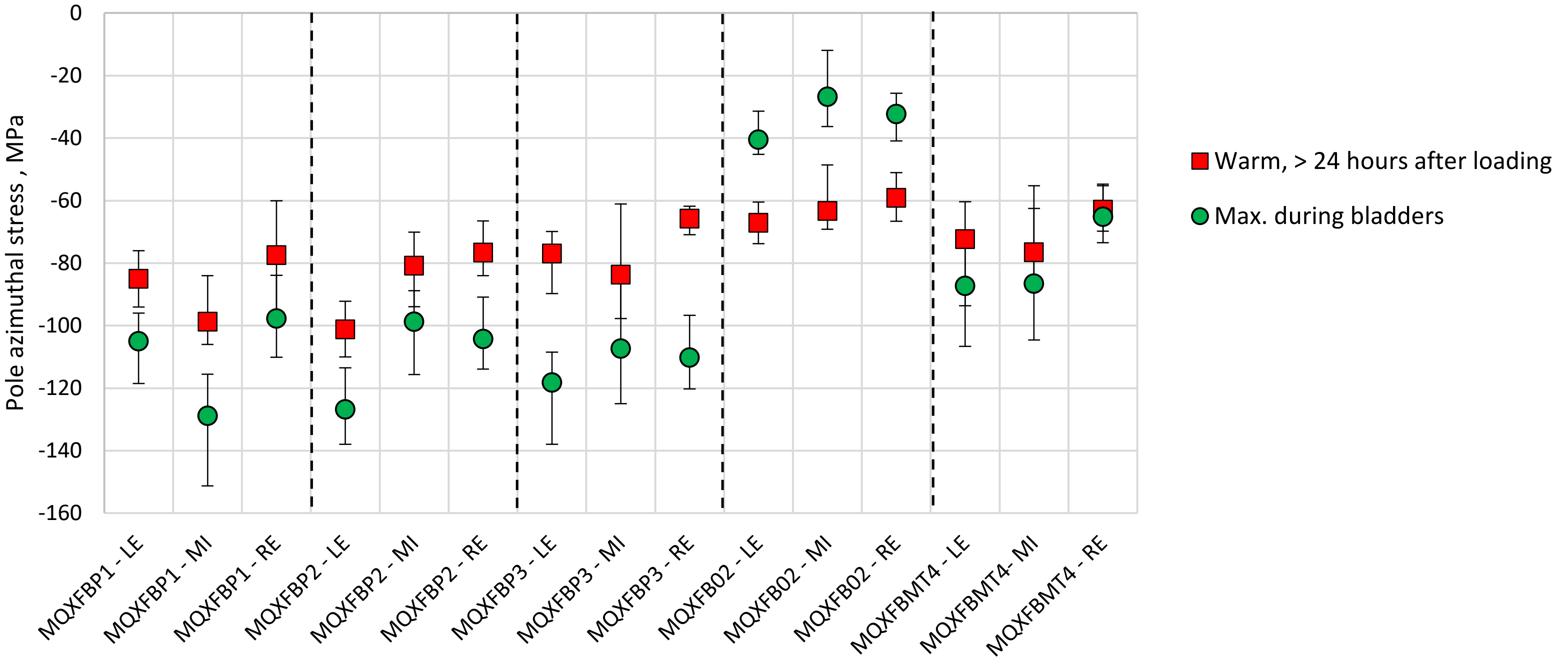

MQXFBMT4 – Assembly

- **Improved alignment** of the mechanical **structure following** the **lessons learnt** from **MQXFBP3** (already implemented in MQXFB02 and MQXFBMT3).

- View from the top (alignment in the horizontal axis):

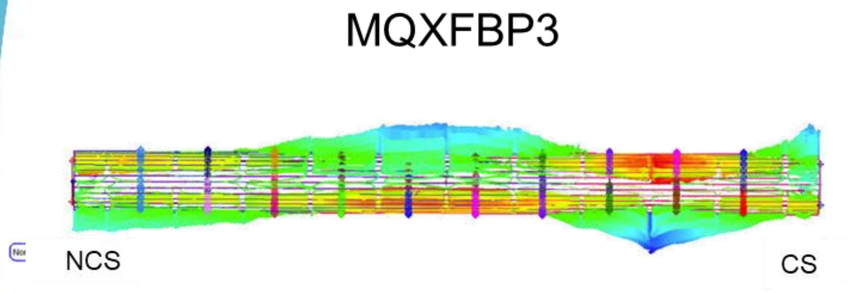

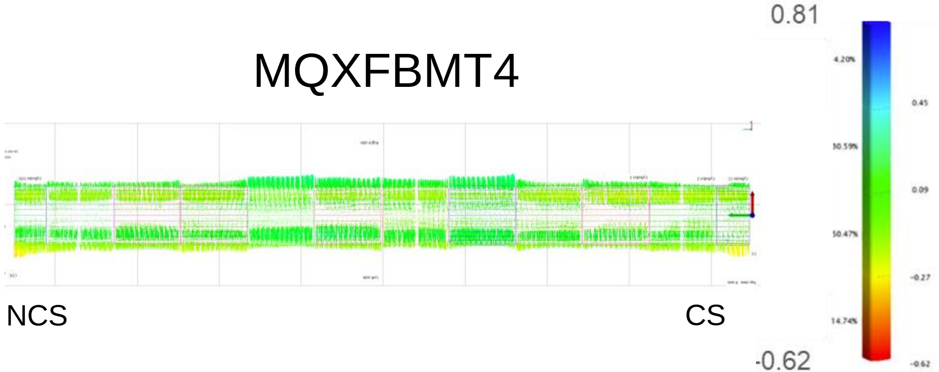

S. Straarup, M. Parent

CONTENTS

- MQXFB:
  - MQXFB02 Cold test results (Focus on mechanics)
  - Highlights on MQXFBMT4 magnet assembly

- MQXFS:
  - **MQXFS7g magnet assembly.**
  - MQXFS8 magnet assembly.

Before MQXFS7g…

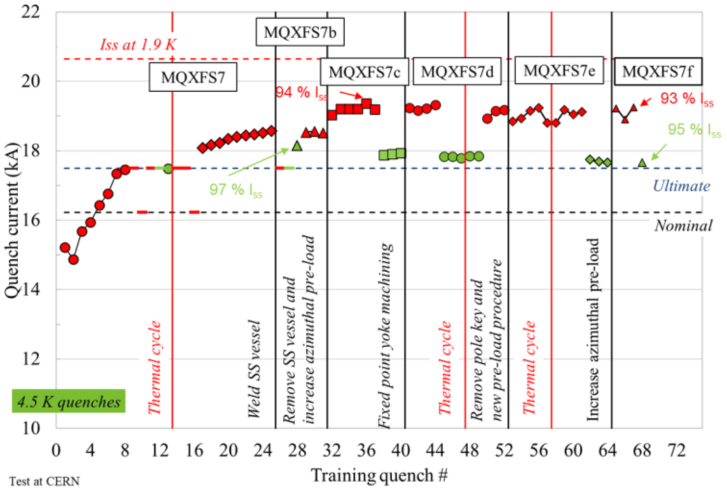

Data: Salvador Ferradas Troitino, Franco Mangiarotti

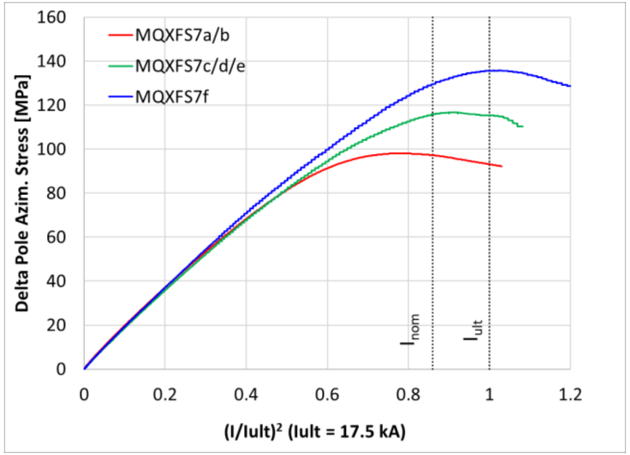

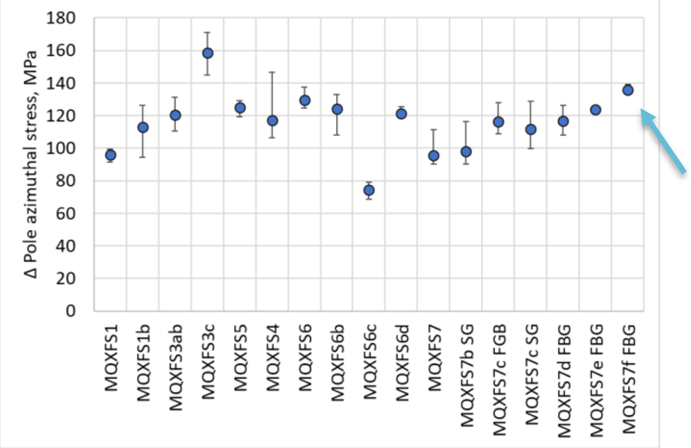

- Pre-load at cold ≈ 140 MPa
- As expected, increase on pole azimuthal stress of 20 MPa

MQXFS7g – Assembly

- New iteration on MQXFS7, **increasing** by **0.1 mm** the thickness of the loading keys (to 14 mm)
- Tubular **bladders re-used** from MQXFS8 (**flattened**).
- Bladder **failure** at **400 bar**, when inserting the **last** 14 mm **key**. Contrary to MQXFBMT4, one **key missing** all **along** the magnet **length.**
- Measured peak az. stress ~ 145 MPa. **Large** coil **imbalance** upon **completion** of the **pre-load**.
- NCR for the bladder failure in progress.

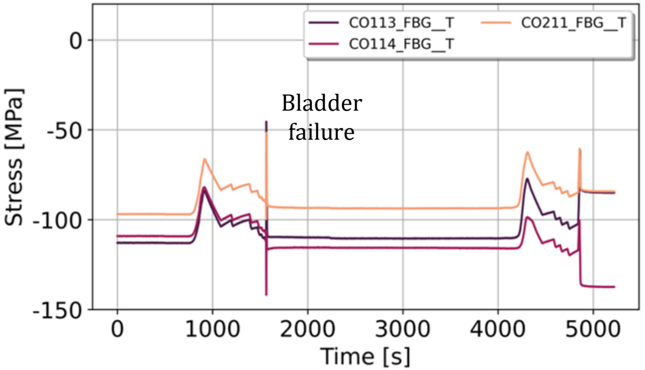

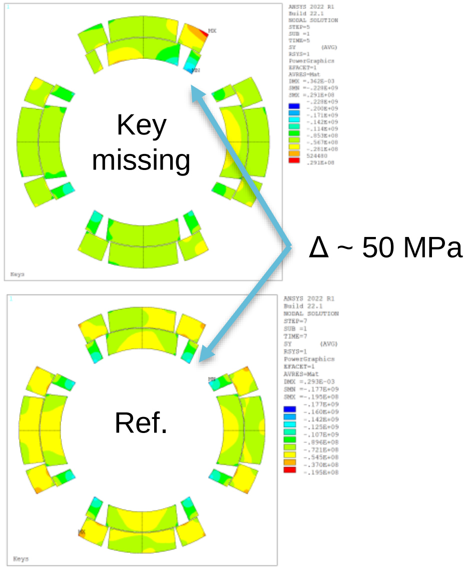

2D FE simulations for the failure case

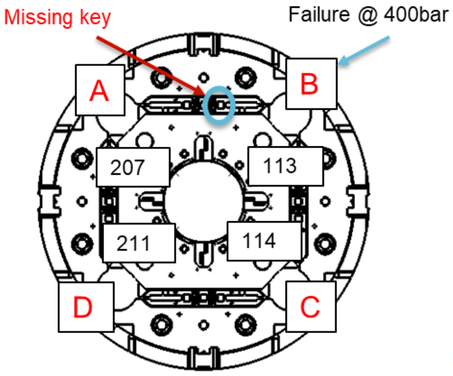

Position of the damaged bladder and the coils in the assembly (LE view).

MQXFS7g – Assembly

- In this case, the **bladder failure** mode **seems** to be **related** with a potential **weakness** induced by the **re-flattening** of already used bladders. Note that bladder stroke in the cooling hole channels is large.
- Furthermore, 14 mm keys are obtained by shimming 13.5 mm keys with additional 0.5 mm. Difficult key insertion. **Time under pressure** was relatively **long**.
- For long MQXFB magnets, bladders are re-used only for disassembly. In this case, they are not re-laminated. Instead, thinner shims are used.
- **Failure mechanism** has been **identified** for **MQXFBMT4** and **MQXFS7g**. **Corrective actions** will be adopted to **minimize** the **risk** of failure in the **future**.

CONTENTS

- MQXFB:
  - MQXFB02 Cold test results (Focus on mechanics)
  - Highlights on MQXFBMT4 magnet assembly

- MQXFS:
  - MQXFS7g magnet assembly.
  - **MQXFS8 magnet assembly.**

MQXFS8 – Assembly

- **MQXFS8** assembled with **2 non-virgin** and **2 virgin** coils.
- All **new** tubular **bladders** used. Same procedure as MQXFB.
- **Centering** and **loading** went extremely **smoothly**.
- Pre-loading **within specifications** (rods not shown for simplicity).

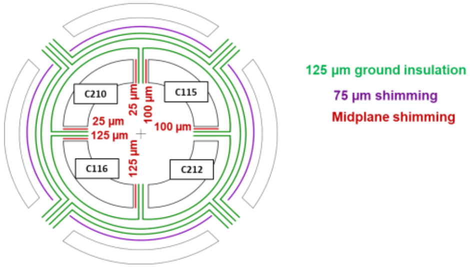

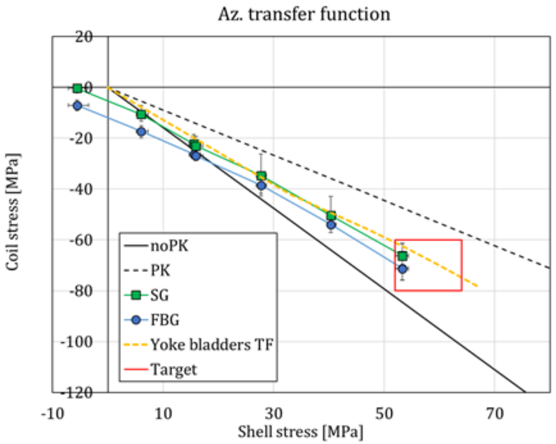

Coils

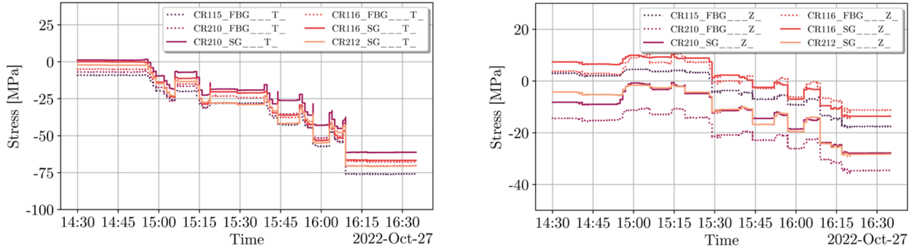

Shell

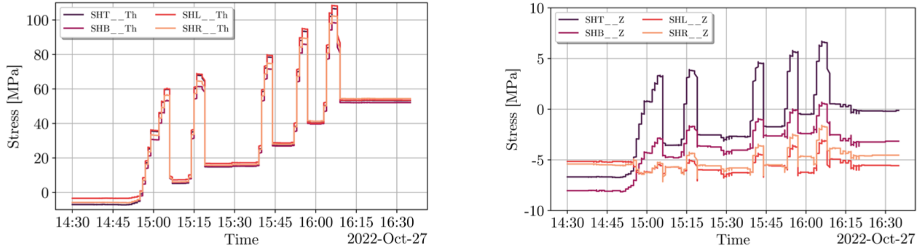

Thank you for your attention!

ANNEX

MQXFB02: Coil Size

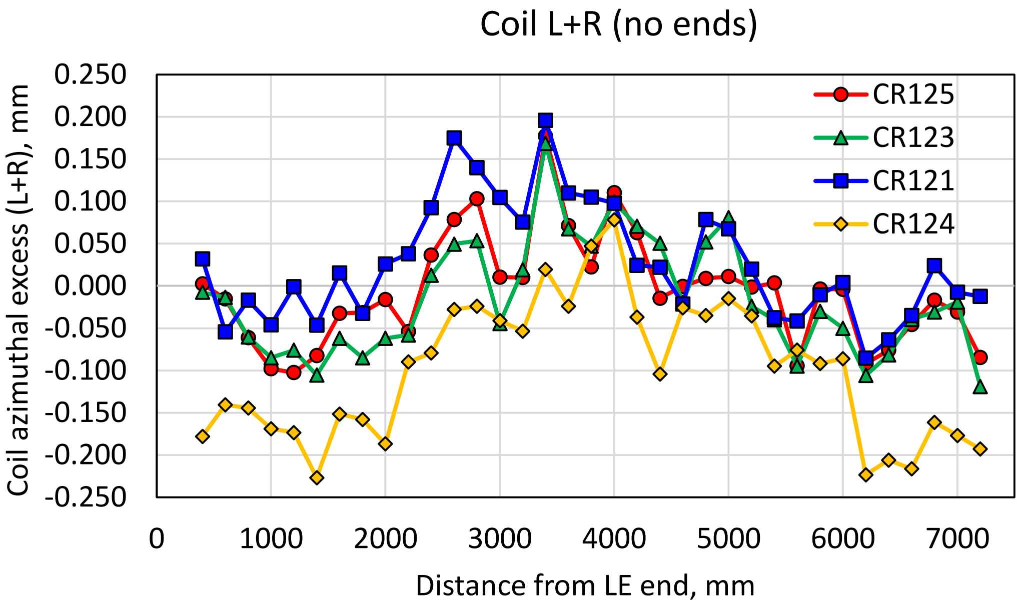

		Average (Including ends)	Average (Excluding ends)
Azimuthal excess L+R [µm]	**CR125**	-39	-7 **(0)**
	CR123	-51	-16 **(0)**
	CR121	-5	27 **(+50)**
	CR124	-117	-100 **(-100)**

	Shim
CR125	**50**
CR123	**50**
CR121	**0**
CR124	**150**

MQXFB02 -250 um shimming plan

Azimuthal size and expected stress variation along the length (w.r.t. average)

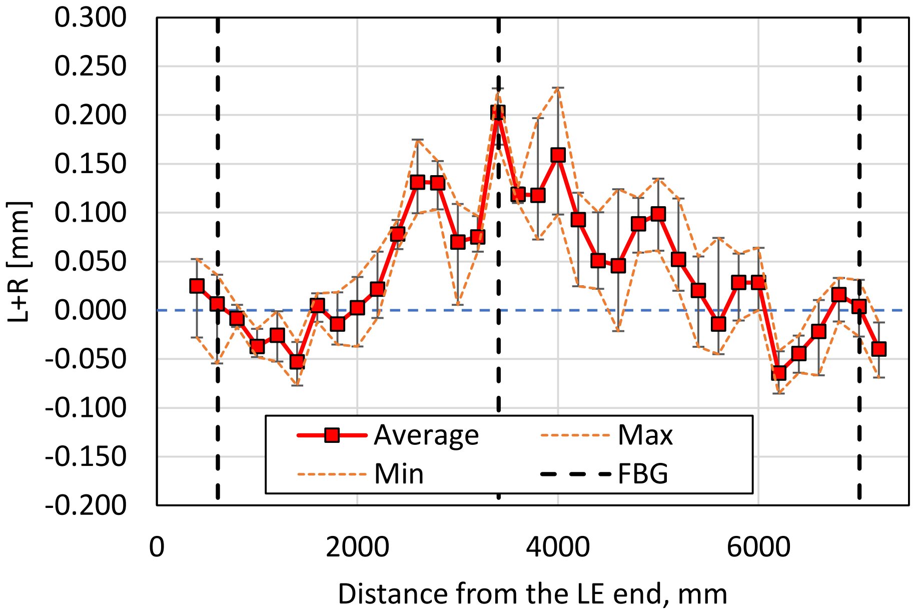

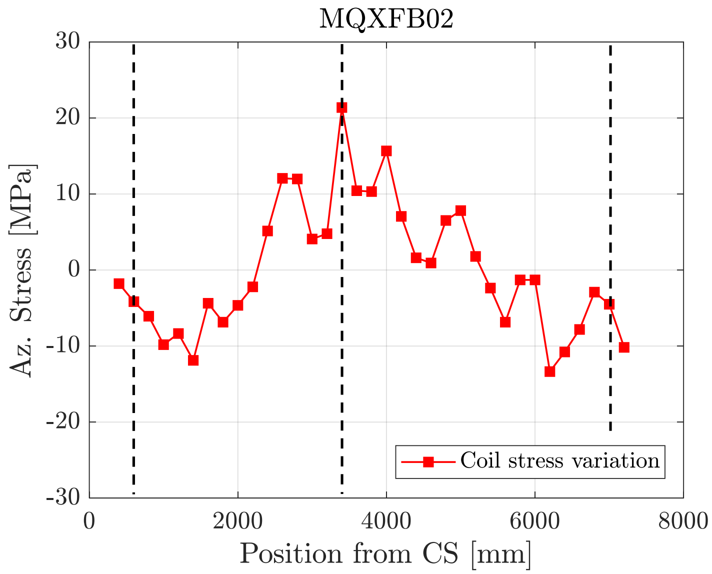

HiLumi HL-LHC PROJECT
CERN
US HL-LHC AUP

MQXFBMT4 – Assembly

- "Tricky coilpack". **FUJI tests confirmed** the expected **mechanical contact** with the **collars**:
  - Larger contact towards the mid-plane for the virgin coil (CR 127). For the non-virgin coils, contact mostly towards the winding pole.
  - The geometry of the new coil is "round". The three tested coils have the typical "squarish" geometry after test.

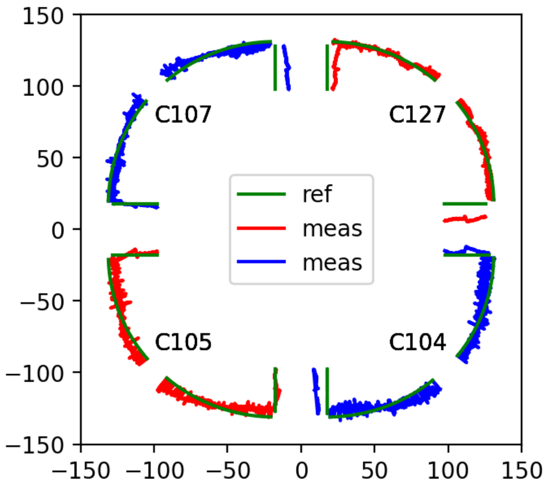

After test:

Before test:

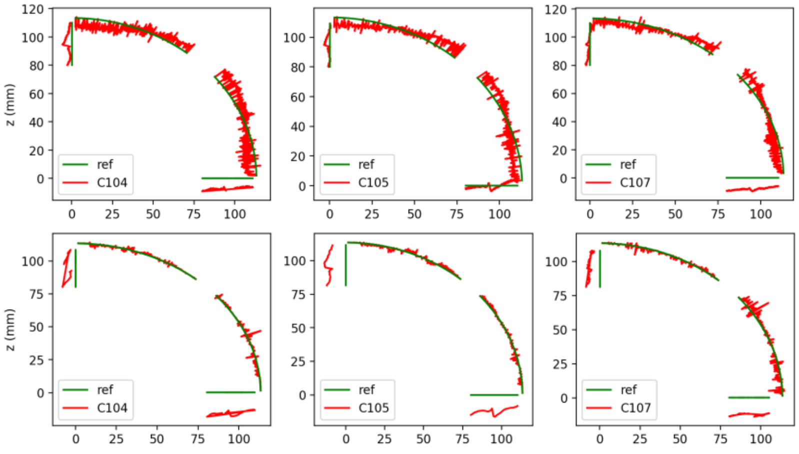

*Same behavior observed for MQXFS8 magnet (2 virgin / 2 non-virgin coils)

MQXFB02 – Cold tests

- Quick recap: cold-mass welding preparation

Gain in azimuthal pole stress during welding: [0 MPa -5 MPa]

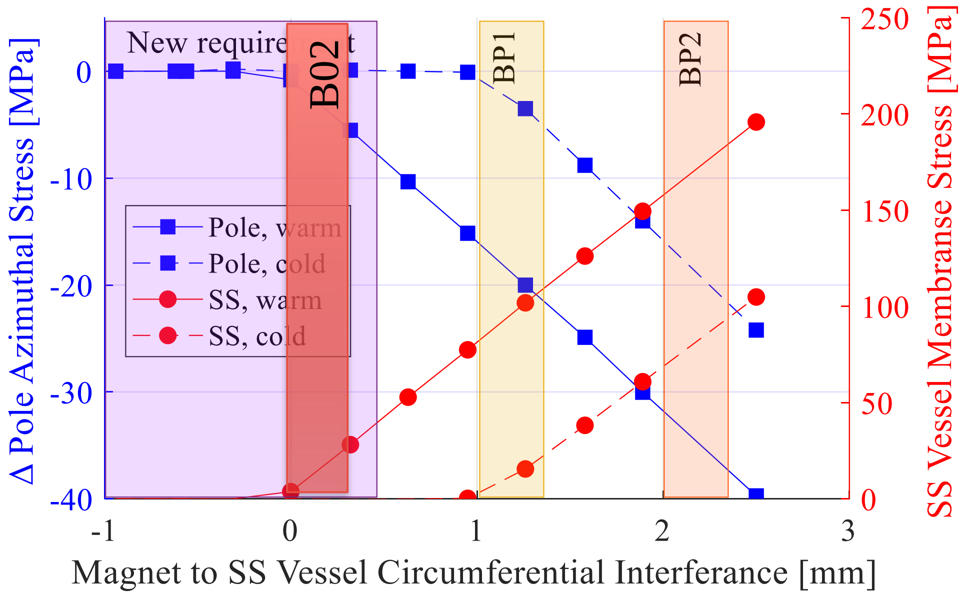

MQXFB02 – Cold tests

- Quick recap: cold-mass welding preparation

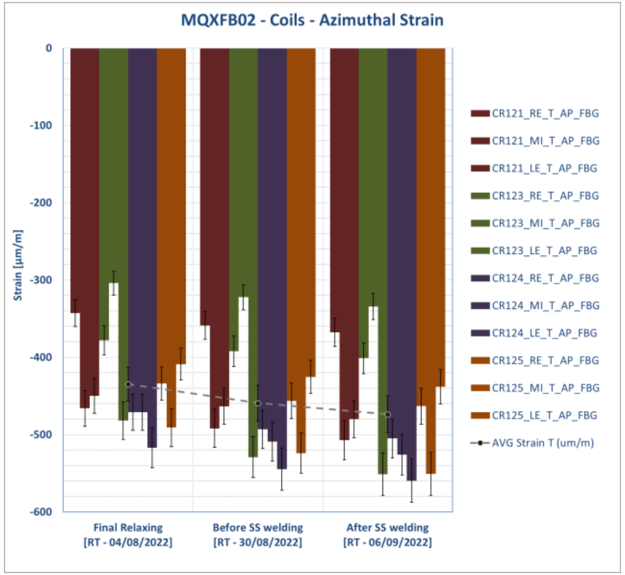

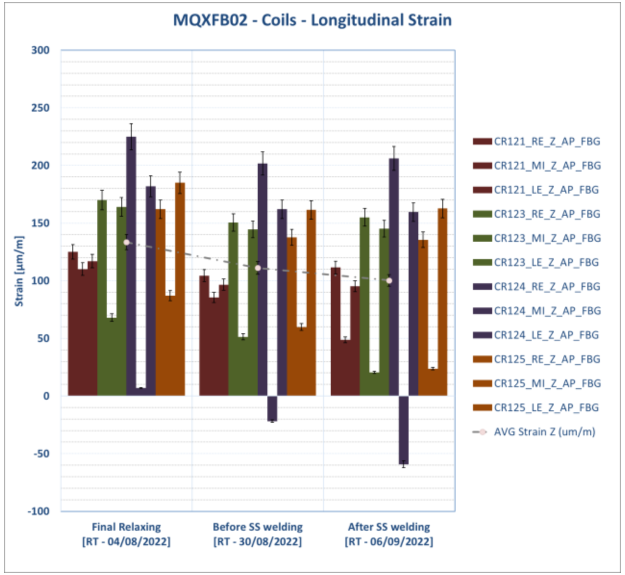

Bladder pressure

2 bladder cycles up to the same pressure to try to recover the imbalance created by the bladder failure

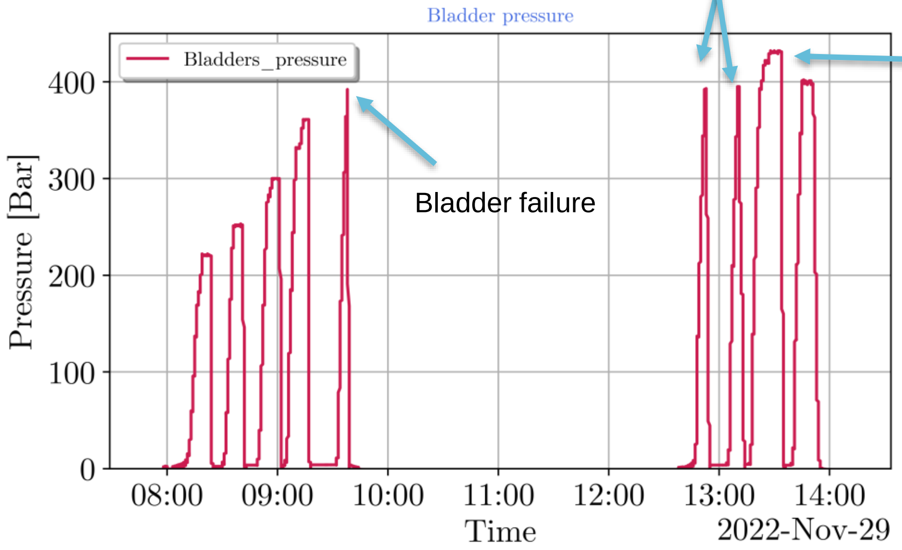

Non-conform keys. Thicker than 13.8 mm and shorter in length.

Bladder failure (LE)

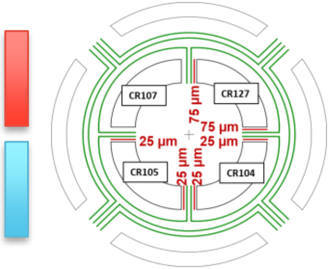

When the bladder failed, 13.7 mm keys were placed in all quadrants. We were just creating the necessary gap to introduce 13.8 mm.

Coil strain

LE - ε_θ

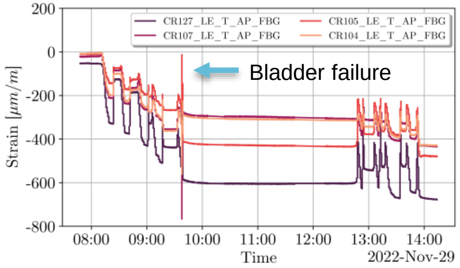

MI - ε_θ

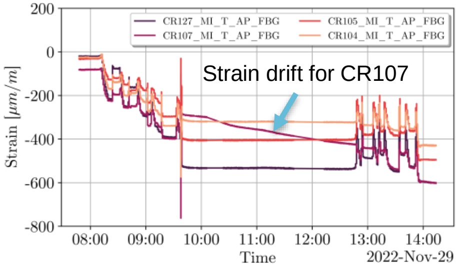

RE - ε_θ

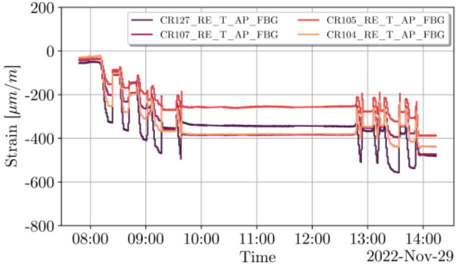

LE - ε_z

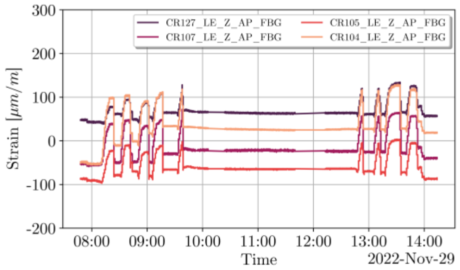

MI - ε_z

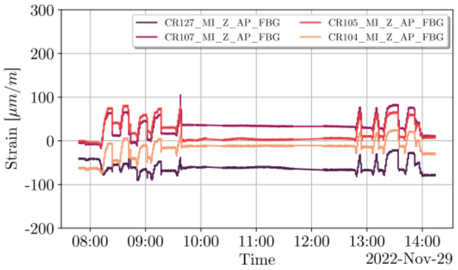

RE - ε_z

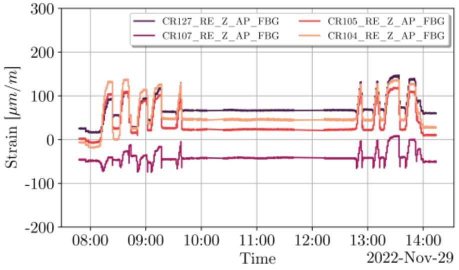

The bladder failure effect (happening in the LE side) is seen in the LE and MI stations.
In these two stations, the failure creates an imbalance among coils. CR127 is the most affected (virgin).

Shell strain

LE - ε_θ

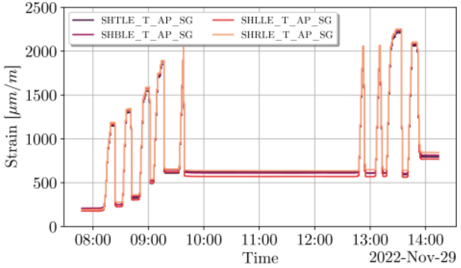

MI - ε_θ

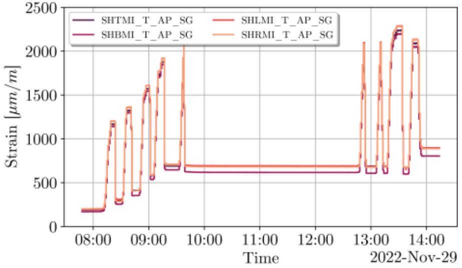

RE - ε_θ

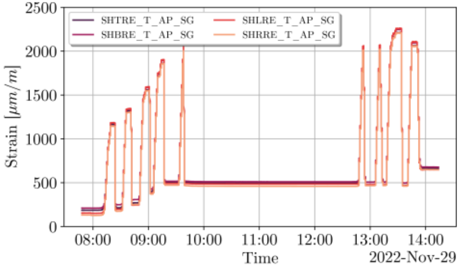

LE - ε_z

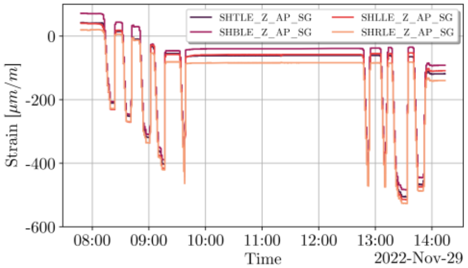

MI - ε_z

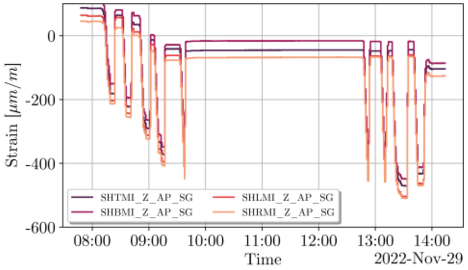

RE - ε_z

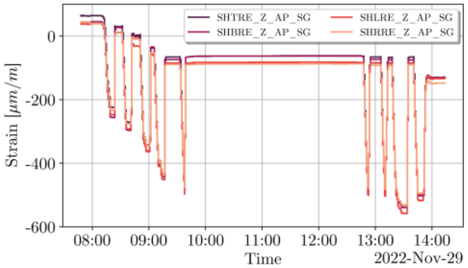

Coil stress

LE - σ_θ

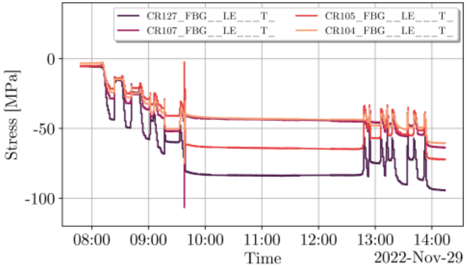

MI - σ_θ

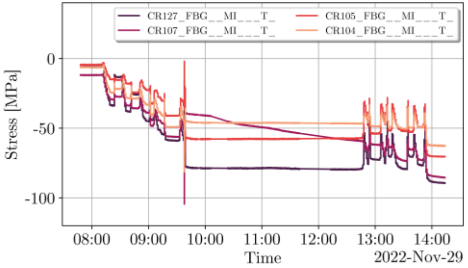

RE - σ_θ

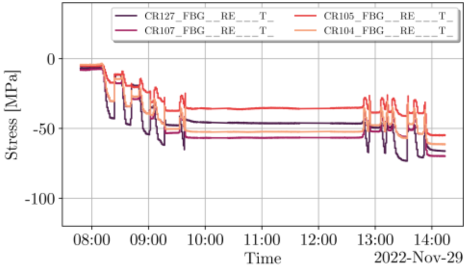

LE - σ_z

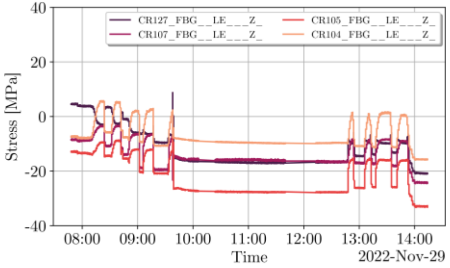

MI - σ_z

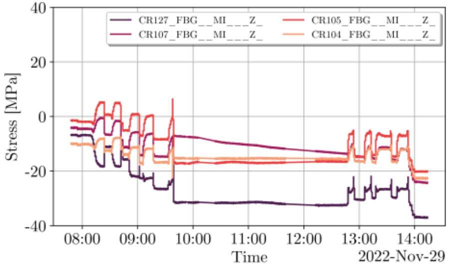

RE - σ_z

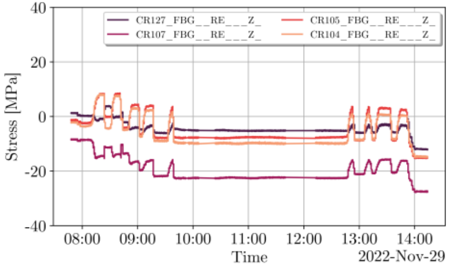

Transitory peak above 100 MPa for CR107, which saw already larger stress levels during MQXFBP1 assembly.

Shell stress

LE - σ_θ

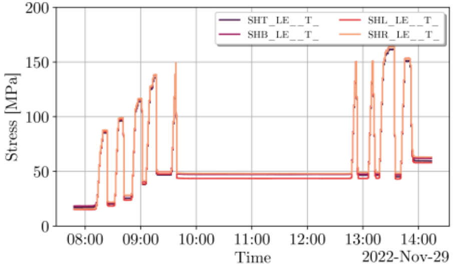

MI - σ_θ

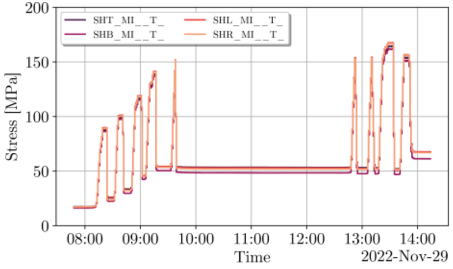

RE - σ_θ

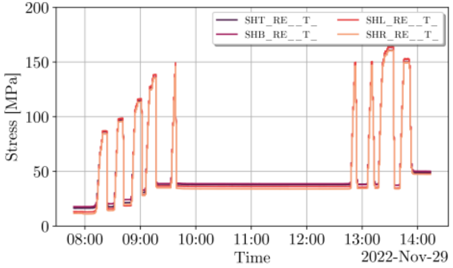

LE - σ_z

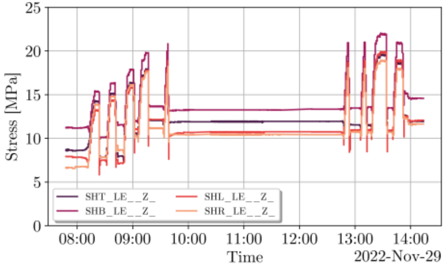

MI - σ_z

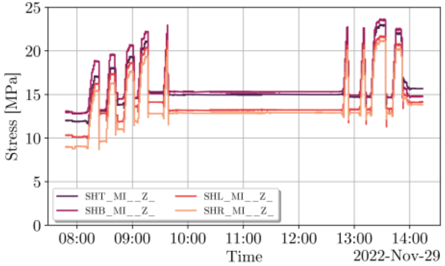

RE - σ_z

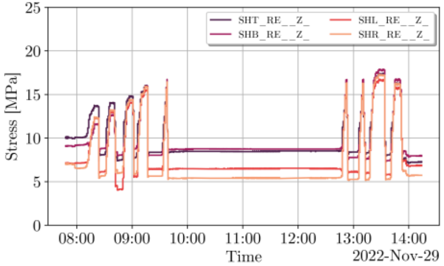

Loading: Coil behavior during bladder bursting

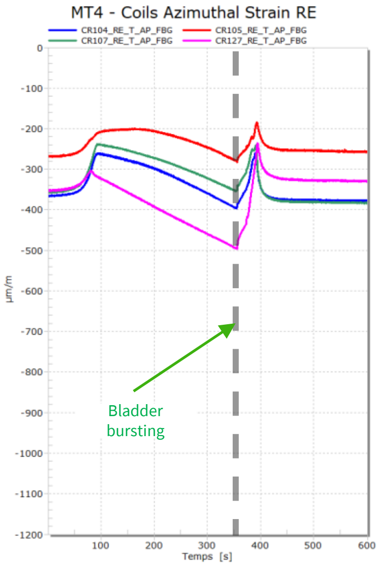

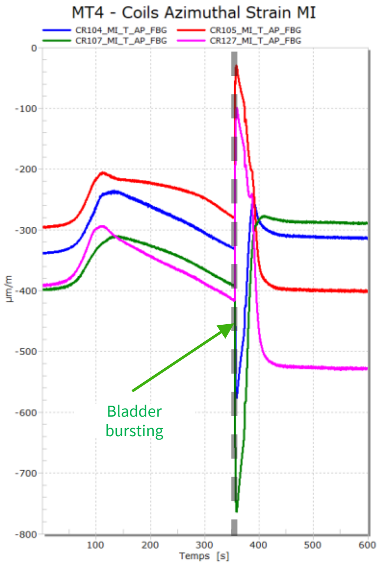

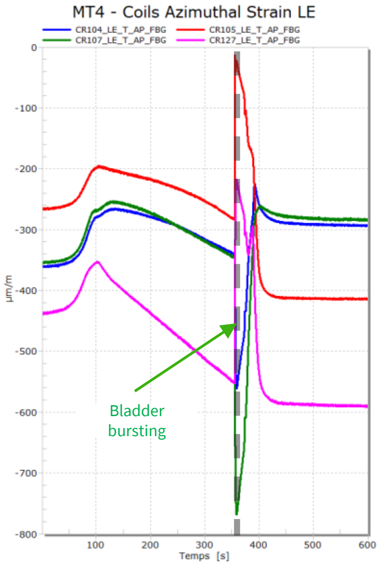

→ Peak strain during bladder bursting: -768 µm/m

Engineering Department

MQXFBMT4 – Assembly

- Two bladder cycles up to 390 Bar performed upon restart of the pre-loading operations. Half of the created imbalance among coils could be recovered.

- Loading completed with the insertion of 13.8 mm keys. Magnet is within specifications except for the coil peak stress. The latter happens in CR107, which has already seen larger stress values during MQXFBP1 assembly and cold test.
  - **Average shell** stress (three stations): 58 MPa - Target: **+58** ± 6 MPa
  - **Average coil stress** (winding pole, three stations): -71 MPa - Target **-70** ± 10 MPa
  - **Peak coil stress** (winding pole, three stations): -107 MPa - Target **-100 MPa**

- As in MQXFBP1 and MQXFBMT2, a large drift in the FBG strain measurements follows after finishing the magnet pre-load. Understanding on-going, but drift and absolute strain values are considered non-critical.
  - In MQXFBMT2 it was proven that such a drift only happened for FBG (SGs, also present, were stable). Once unloaded, the offset remained in the strain readings.
  - Drift does not happen after bladder failure in short models. Inhomogeneous FBG loading along the length?
  - Interestingly, both in BP1 and MT4 the strain stabilizes at the same value. To be continued…

Before MQXFS7g…

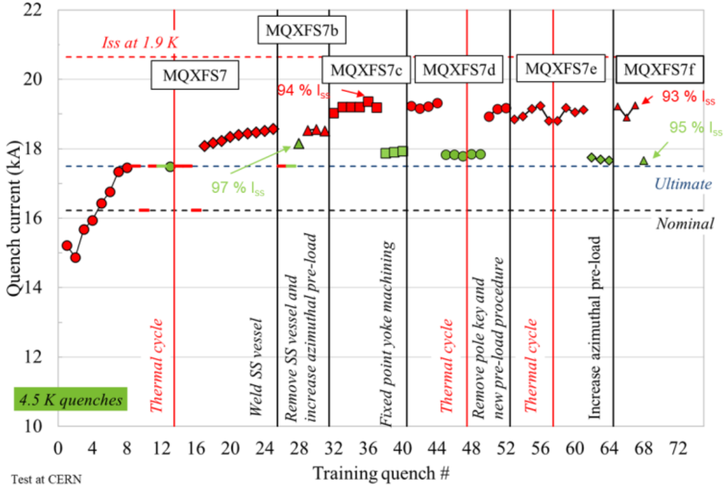

Data: Salvador Ferradas Troitino, Franco Mangiarotti

S7f

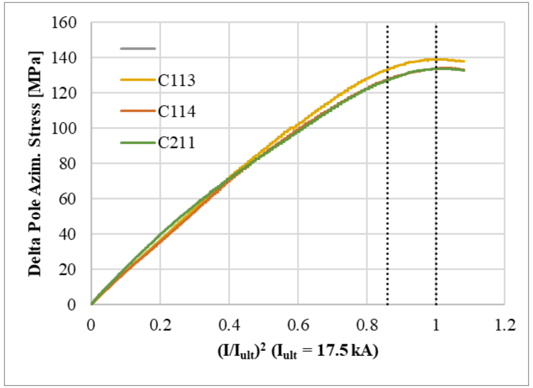

- Pre-load at cold ≈ 140 MPa
- As expected, increase on pole azimuthal stress of 20 MPa

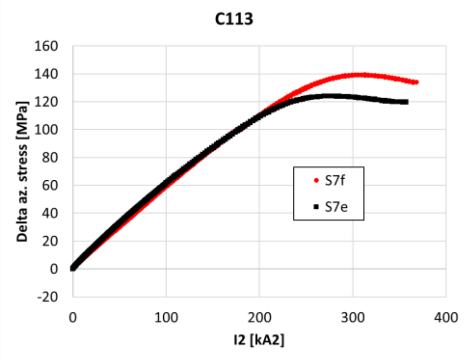

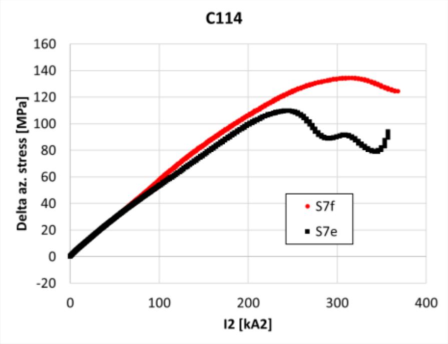

Rods

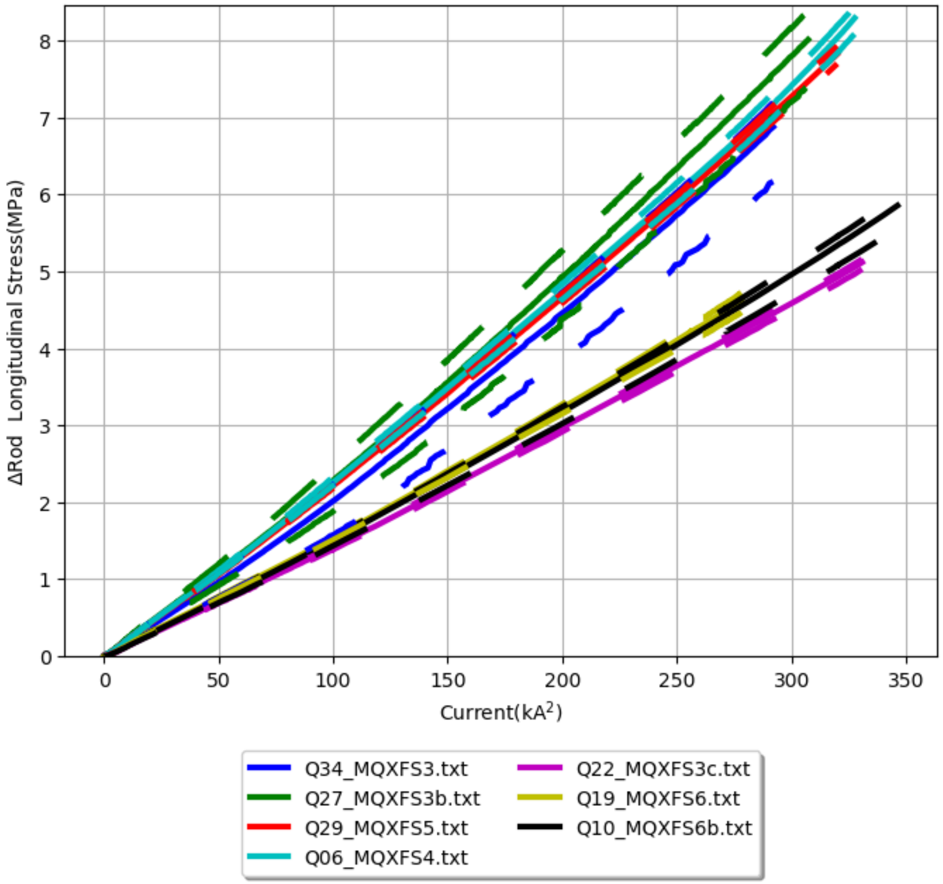

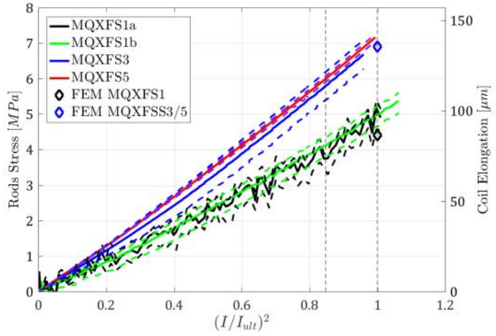

(c)

Fig. 7. Strain gauge measurements during magnet powering. (a) Comparison of measured delta pole azimuthal stress: average (continuous lines) and variation across the quadrants (dashed lines). (b) Delta azimuthal stress on the shell. The auxiliary y-axis on the right shows the radius variation extracted from the strain. (c) Delta stress on the rods, along with the equivalent total coil elongation on the auxiliary y-axis.

MQXFB rods

Rod relative behaviour during powering: Difference between FEM and measurements is roughly 2.5 fold.

In previous studies, a change of friction coefficient of coil to collar surface from 0.16 to 0.13 led to a change in delta rod stress from 4.4 MPa to 6.9 MPa.

Changing the friction coefficient in the current reference model between 0.2 and 0.3 doesn’t seem to lead to a large change in delta rod stress. A coefficient of 0.16 seems already low (laminated aluminium, polyimide surface).

Instead, a variation of the axial elastic modulus in orthotropic approximation was tried for the laminated yoke. The modulus had to be lowered down to 40% (90 GPa) of the original in order to match the measured values.

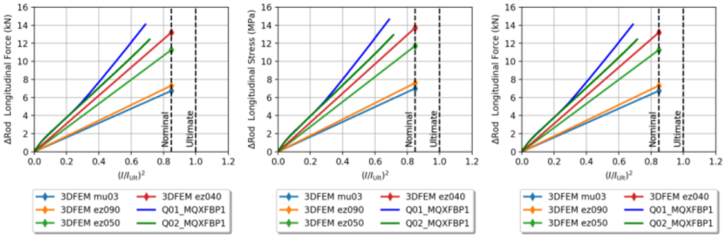

Figure 22: Rods vs normalized current squared: comparison of the measured values and computed values. 3D FE models are computed with 0.3 friction and varying axial elastic modulus using orthotropic yoke material approximation. The rod force at nominal current is 1.17 MN; large portion of it is held by the friction.

Table 4: Rod comparison of different MQXF magnets at nominal current. Thin and thick refer to the lamination type. MQXFB values are extrapolated.

Magnet type	$\Delta\varepsilon$ (µe)	$\Delta\sigma$ (MPa)	ΔF_{rod} (kN)	$\Delta F_{\mathrm{axial}}$ (kN)	$\Delta F_{\mathrm{axial}}/F_{\mathrm{em,nom}}$ (%)	Δl (µm)
MQXFS thick	56	4.4	4.5	18	1.5	84
MQXFS thin	85	6.7	6.8	27	2.3	127
MQXFA	64	14	13	52	4.4	290
MQXFB	79	17	16	64	5.5	590

Rods

MQXFB - RODS					
S	XG	YG	ZG	EZ	SZ
0.00E+00	9.72E-02	9.72E-02	3.76E+00	6.23E-04	1.20E+08
2.48E-02	1.22E-01	9.72E-02	3.76E+00	6.05E-04	1.17E+08
4.95E-02	1.22E-01	1.22E-01	3.76E+00	5.87E-04	1.13E+08
Average				6.05E-04	1.17E+08
				605	117
				µstr	MPa

MQXFB - RODS COLD					
S	XG	YG	ZG	EZ	SZ
0.00E+00	9.72E-02	9.72E-02	3.76E+00	1.36E-03	2.86E+08
2.48E-02	1.22E-01	9.72E-02	3.76E+00	1.27E-03	2.67E+08
4.95E-02	1.22E-01	1.22E-01	3.76E+00	1.19E-03	2.49E+08
Average				1.27E-03	2.67E+08
				1273	267
				µstr	MPa

MQXFB - RODS POWERING					
S	XG	YG	ZG	EZ	SZ
0.00E+00	9.72E-02	9.72E-02	3.76E+00	1.40E-03	2.93E+08
2.48E-02	1.22E-01	9.72E-02	3.76E+00	1.31E-03	2.75E+08
4.95E-02	1.22E-01	1.22E-01	3.76E+00	1.22E-03	2.56E+08
Average				1.31E-03	2.75E+08
				1308	275
				µstr	MPa

DELTA CD
669

DELTA POWERING
35

MQXFS – Experience from short magnets

- As expected from the model, the rods only see 2 % for the electromagnetic forces during powering
- Small differences observed in between the two types of structures:
  - Structure 1&2 (thick laminations, large gap coil to collar): 1.4 % of F_{emz} in the rods, 0.16 friction coefficient needed to match the measurements
  - Structure 3 (thin laminations, small gap coil to collar): 2.2 % of F_{emz} in the rods, 0.13 friction coefficient needed to match the measurements
- Measurements confirm that coil elongation is independent of the pre-load level, since it depends on the system stiffness. The effect of the pre-load is to increase the contact pressure coil to pole in the end region.

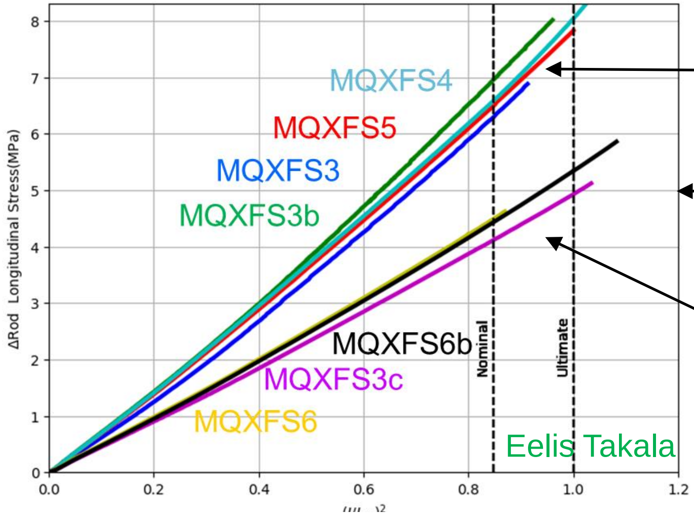

Thin laminations, 5*0.125 mm gap between coil and collar, filled with polyimide

5 MPa ≈ 0.1 mm of coil elongation

Thick laminations, 13*0.125 mm gap between coil and collar, filled with polyimide or G10

G. Vallone, et. al., Mechanical analysis of the short model magnets for the Nb_3Sn low-beta quadrupole MQXF, *IEEE Trans. Appl. Supercond.*, vol. 26, no. 4, 2016.